

# UPDATE ON MINIMAL SUPERSYMMETRIC HYBRID INFLATION IN LIGHT OF PLANCK

CONSTANTINOS PALLIS<sup>1</sup> AND QAISAR SHAFI<sup>2</sup>

<sup>1</sup>*Department of Physics, University of Cyprus, P.O. Box 20537, Nicosia 1678, CYPRUS*

*e-mail address: cpallis@ucy.ac.cy*

<sup>2</sup>*Bartol Research Institute, Department of Physics and Astronomy, University of Delaware, Newark, DE 19716, USA*

*e-mail address: shafi@bartol.udel.edu*

**ABSTRACT:** The minimal supersymmetric (or F-term) hybrid inflation is defined by a unique renormalizable superpotential, fixed by a  $U(1)$  R-symmetry, and it employs a canonical Kähler potential. The inflationary potential takes into account both radiative and supergravity corrections, as well as an important soft supersymmetry breaking term, with a mass coefficient in the range  $(0.1 - 10)$  TeV. The latter term assists in obtaining a scalar spectral index  $n_s$  close to 0.96, as strongly suggested by the PLANCK and WMAP-9yr measurements. The minimal model predicts that the tensor-to-scalar  $r$  is extremely tiny, of order  $10^{-12}$ , while the spectral index running,  $|dn_s/d\ln k| \sim 10^{-4}$ . If inflation is associated with the breaking of a local  $U(1)_{B-L}$  symmetry, the corresponding symmetry breaking scale  $M$  is  $(0.7 - 1.6) \cdot 10^{15}$  GeV with  $n_s \simeq 0.96$ . This scenario is compatible with the bounds on  $M$  from cosmic strings, formed at the end of inflation from  $B - L$  symmetry breaking. We briefly discuss non-thermal leptogenesis which is readily implemented in this class of models.

PACs numbers: 98.80.Cq, 12.60.Jv

## I. INTRODUCTION

*Supersymmetric* (SUSY) hybrid inflation based on F-terms, also referred to as *F-term hybrid inflation* (FHI), is one of the simplest and well-motivated inflationary models [1, 2]. It is tied to a renormalizable superpotential uniquely determined by a global  $U(1)$  R-symmetry, does not require fine tuned parameters, and it is naturally associated with the breaking of a local symmetry, such as  $G_{B-L} = G_{\text{MSSM}} \times U(1)_{B-L}$  [3], where  $G_{\text{MSSM}} = SU(3)_C \times SU(2)_L \times U(1)_Y$  is the gauge group of the *Minimal Supersymmetric Standard Model* (MSSM) or,  $G_{\text{LR}} = SU(2)_L \times SU(2)_R \times U(1)_{B-L}$  [4], flipped  $SU(5)$  [5], etc. As shown in Ref. [1], the addition of *radiative corrections* (RCs) to the tree level inflationary potential predicts a scalar spectral index  $n_s \simeq 0.98$ , and the microwave temperature anisotropy  $\Delta T/T$  is proportional to  $(M/m_P)^2$ , where  $M$  denotes the scale of the gauge symmetry breaking. It turns out that  $M$  usually is not far from  $M_{\text{GUT}} \simeq (2 - 3) \cdot 10^{16}$  GeV. Here  $m_P = 2.4 \cdot 10^{18}$  GeV is the reduced Planck mass. A more complete treatment [6], which incorporates *supergravity* (SUGRA) corrections [7] with canonical (minimal) Kähler potential, as well as an important soft SUSY breaking term [8], can yield lower  $n_s$  values (0.95 – 0.97). Recall that the minimal Kähler potential insures that the SUGRA corrections do not spoil the flatness of the potential that is required to implement FHI – reduction of  $n_s$  by invoking non-minimal Kähler potentials is analyzed in Ref. [9–11].

Insisting on the simplest realization of FHI – and the one-step inflationary paradigm, cf. Ref. [12] – we wish to emphasize here that FHI is in good agreement, in a rather narrow but well-defined range of its parameters, with the latest WMAP [13] and PLANCK [14] data pertaining to the  $\Lambda$ CDM framework. To this end, SUGRA [7] and soft SUSY breaking [6, 8] corrections are taken into account, in addition to the well-known [1] RCs. The minimality of the model is justified by the fact that FHI is implemented within *minimal supergravity* (mSUGRA) and within a minimal extension of  $G_{\text{MSSM}}$ , obtained by promoting the pre-existing global  $U(1)_{B-L}$  sym-

metry of MSSM to a local one. As a consequence, three *right-handed neutrinos*,  $\nu_i^c$ , are necessary to cancel the anomalies. The presence of  $\nu_i^c$  leads to a natural explanation for the observed [15] *baryon asymmetry of the universe* (BAU) via *non-thermal leptogenesis* (nTL) [16], and the existence of tiny but non-zero neutrino masses. As we show, this set-up is compatible with the gravitino constraint [17, 18] and the current data [19, 20] on the neutrino oscillation parameters. It is worth mentioning that our scenario fits well with the bound [21] induced by the non-observation of the cosmic strings, formed during the  $B - L$  phase transition. Note that strings may serve as a source [22] of a controllable amount of non-gaussianity in the cosmic microwave background anisotropy.

In the following discussion, we briefly review the minimal FHI and present our updated results in Sec. II. We then consider nTL using updated constraints from neutrino physics in Sec. III. Our conclusions are summarized in Sec. IV.

## II. MINIMAL FHI MODEL

1. **GENERAL SET-UP.** The minimal FHI is based on the superpotential

$$W_{\text{HI}} = \kappa S (\bar{\Phi}\Phi - M^2), \quad (1)$$

where  $\bar{\Phi}$ ,  $\Phi$  denote a pair of chiral superfields oppositely charged under  $U(1)_{B-L}$ ,  $S$  is a  $G_{B-L}$ -singlet chiral superfield, and the parameters  $\kappa$  and  $M$  are made positive by field redefinitions.  $W_{\text{HI}}$  is the most general renormalizable superpotential consistent with a continuous R-symmetry [1] under which  $S \rightarrow e^{i\alpha} S$ ,  $\bar{\Phi}\Phi \rightarrow \bar{\Phi}\Phi$ ,  $W \rightarrow e^{i\alpha} W$ . The SUSY potential,  $V_{\text{SUSY}}$ , extracted (see e.g. Ref. [23, 24]) from  $W_{\text{HI}}$  in Eq. (1) includes F and D-term contributions. Along the direction  $|\bar{\Phi}| = |\Phi|$ , the latter contribution vanishes whereas the former reads

$$V_{\text{SUSY}} = \kappa^2 (|\Phi|^2 - M^2)^2 + 2|S|^2|\Phi|^2. \quad (2)$$

The scalar components of the superfields are denoted by the same symbols as the corresponding superfields. Restricting

ourselves to the D-flat direction, from  $V_{\text{SUSY}}$  in Eq. (2) we find that the SUSY vacuum lies at

$$\langle S \rangle = 0 \quad \text{and} \quad |\langle \Phi \rangle| = |\langle \bar{\Phi} \rangle| = M. \quad (3)$$

As a consequence,  $W_{\text{HI}}$  leads to the spontaneous breaking of  $G_{B-L}$ , to  $G_{\text{MSSM}}$  with SUSY unbroken.

The superpotential  $W_{\text{HI}}$  also gives rise to FHI since, for values of  $|S| \gg M$ , there exist a flat direction

$$\bar{\Phi} = \Phi = 0 \quad \text{with,} \quad V_{\text{SUSY}} (\bar{\Phi} = \Phi = 0) \equiv V_{\text{HI0}} = \kappa^2 M^4. \quad (4)$$

Thus,  $V_{\text{HI0}}$  provides us with a constant potential energy density which can be used to implement FHI.

2. THE INFLATIONARY POTENTIAL. To a good approximation, the inflationary potential of minimal FHI can be written as

$$V_{\text{HI}} = V_{\text{HI0}} + V_{\text{Hlc}} + V_{\text{HIS}} + V_{\text{HIT}}, \quad (5)$$

where, besides the dominant contribution  $V_{\text{HI0}}$  in Eq. (4),  $V_{\text{HI}}$  includes the following contributions:

- $V_{\text{Hlc}}$  represents the RCs to  $V_{\text{HI}}$  originating from a mass splitting in the  $\Phi - \bar{\Phi}$  supermultiplets, caused by SUSY breaking along the inflationary valley [1]:

$$V_{\text{Hlc}} = \frac{\kappa^2 N}{32\pi^2} V_{\text{HI0}} \left( 2 \ln \frac{\kappa^2 x M^2}{Q^2} + f_{\text{rc}}(x) \right), \quad (6a)$$

where  $N = 1$  is the dimensionality of the representations to which  $\bar{\Phi}$  and  $\Phi$  belong,  $Q$  is a renormalization scale,  $x = \sigma^2/2M^2$  with  $\sigma = \sqrt{2}|S|$  being the canonically normalized inflaton field, and

$$f_{\text{rc}}(x) = (x+1)^2 \ln(1+1/x) + (x-1)^2 \ln(1-1/x). \quad (6b)$$

- $V_{\text{HIS}}$  is the SUGRA correction to  $V_{\text{HI}}$  [7, 8]:

$$V_{\text{HIS}} = V_{\text{HI0}} \sigma^4 / 8m_{\text{P}}^4, \quad (7)$$

where we employ the canonical Kähler potential  $K = |S|^2 + |\Phi|^2 + |\bar{\Phi}|^2$  working within mSUGRA.

- $V_{\text{HIT}}$  is the most important contribution to  $V_{\text{HI}}$  from the soft SUSY effects [6, 8] parameterized as follows:

$$V_{\text{HIT}} = -a_S \sigma \sqrt{V_{\text{HI0}}/2}, \quad (8)$$

where [4, 6]  $a_S = 2|2 - A|m_{3/2} \cos(\theta_S + \theta_{(2-A)})$  is the tadpole parameter, taking values comparable to the gravitino,  $\tilde{G}$ , mass,  $m_{3/2} \sim (0.1 - 10)$  TeV. The soft SUSY breaking mass<sup>2</sup> term for  $S$ , with mass  $\sim m_{3/2}$ , is negligible [10] for FHI. Also,  $A$  is the dimensionless trilinear coupling, of order unity, associated with the first term of  $W_{\text{HI}}$  in Eq. (1). Imposing the condition  $\theta_S + \theta_{(2-A)} = 0 \bmod 2\pi$ ,  $V_{\text{HI}}$  is minimized with respect to (w.r.t.) the phases  $\theta_S$  and  $\theta_{(2-A)}$  of  $S$  and  $(2-A)$  respectively. We further assume that  $\theta_S$  remains constant during FHI.

3. THE INFLATIONARY OBSERVABLES – REQUIREMENTS. Under the assumptions that (i) the curvature perturbation generated by  $\sigma$  is solely responsible for the one that is observed, and (ii) FHI is followed in turn by a decaying-particle, radiation and matter domination, the parameters of our model can be restricted by requiring that:

- The number of e-foldings  $N_{\text{HI}*}$  that the scale  $k_* = 0.05/\text{Mpc}$  undergoes during FHI leads to a solution of the horizon and flatness problems of standard big bang cosmology. Employing standard methods [11, 14, 24], we can derive the relevant condition:

$$N_{\text{HI}*} \equiv \int_{\sigma_f}^{\sigma_*} \frac{d\sigma}{m_{\text{P}}^2} \frac{V_{\text{HI}}}{V'_{\text{HI}}} \simeq 19.4 + \frac{2}{3} \ln \frac{V_{\text{HI0}}^{1/4}}{1 \text{ GeV}} + \frac{1}{3} \ln \frac{T_{\text{rh}}}{1 \text{ GeV}}, \quad (9)$$

where  $T_{\text{rh}}$  is the reheat temperature after FHI, the prime denotes derivation w.r.t.  $\sigma$ ,  $\sigma_*$  is the value of  $\sigma$  when  $k_*$  crossed outside the horizon of FHI, and  $\sigma_f$  is the value of  $\sigma$  at the end of FHI, which can be found, in the slow-roll approximation [24], from the condition

$$\max\{\epsilon(\sigma_f), |\eta(\sigma_f)|\} = 1, \quad \text{where} \\ \epsilon \simeq m_{\text{P}}^2 (V'_{\text{HI}}/V_{\text{HI}})^2 / 2 \quad \text{and} \quad \eta \simeq m_{\text{P}}^2 V''_{\text{HI}}/V_{\text{HI}}. \quad (10)$$

Actually, in our set-up, the slow-roll conditions are violated infinitesimally close to the critical point  $\sigma_c = \sqrt{2}M$  appearing in the particle spectrum of  $\Phi - \bar{\Phi}$  system during FHI.

- The amplitude,  $A_s$ , of the power spectrum of the curvature perturbation, which is generated during FHI and calculated at  $k_*$  as a function of  $\sigma_*$ , is consistent with the data [13, 14], i.e.

$$A_s^{1/2} = \frac{1}{2\sqrt{3}\pi m_{\text{P}}^3} \frac{V_{\text{HI}}^{3/2}(\sigma_*)}{|V_{\text{HI},\sigma}(\sigma_*)|} \simeq 4.685 \cdot 10^{-5}. \quad (11)$$

- The (scalar) spectral index  $n_s$ , its running,  $dn_s/d \ln k \equiv \alpha_s$ , and the scalar-to-tensor ratio,  $r$ , which are given by

$$n_s = 1 - 6\epsilon_* + 2\eta_*, \quad (12a)$$

$$\alpha_s = 2(4\eta_*^2 - (n_s - 1)^2)/3 - 2\xi_* \quad \text{and} \quad r = 16\epsilon_*, \quad (12b)$$

where  $\xi \simeq m_{\text{P}}^4 V'_{\text{HI}} V'''_{\text{HI}} / V_{\text{HI}}^2$  and all variables with the subscript  $*$  are evaluated at  $\sigma = \sigma_*$ , should be in agreement with the following values [13, 14] based on the  $\Lambda$ CDM model:

$$n_s = 0.9603 \pm 0.014 \Rightarrow 0.945 \lesssim n_s \lesssim 0.975, \quad (13a)$$

$$\alpha_s = -0.0134 \pm 0.018, \quad \text{and} \quad r < 0.11, \quad (13b)$$

at 95% confidence level (c.l.).

- The tension  $\mu_{\text{cs}}$  of the  $B - L$  cosmic strings produced at the end of FHI respects the bound [21] – cf. Ref. [25–27]:

$$\mu_{\text{cs}} \approx 4.8\pi M^2 / \ln(2/\beta) \lesssim 8 \cdot 10^{-6} m_{\text{P}}^2. \quad (14)$$

Here, the results of the simulations for the abelian Higgs model are adopted,  $\beta = \kappa^2/2g^2 \leq 10^{-2}$ , with  $g \simeq 0.7$  being the gauge coupling constant close to  $M_{\text{GUT}}$ .

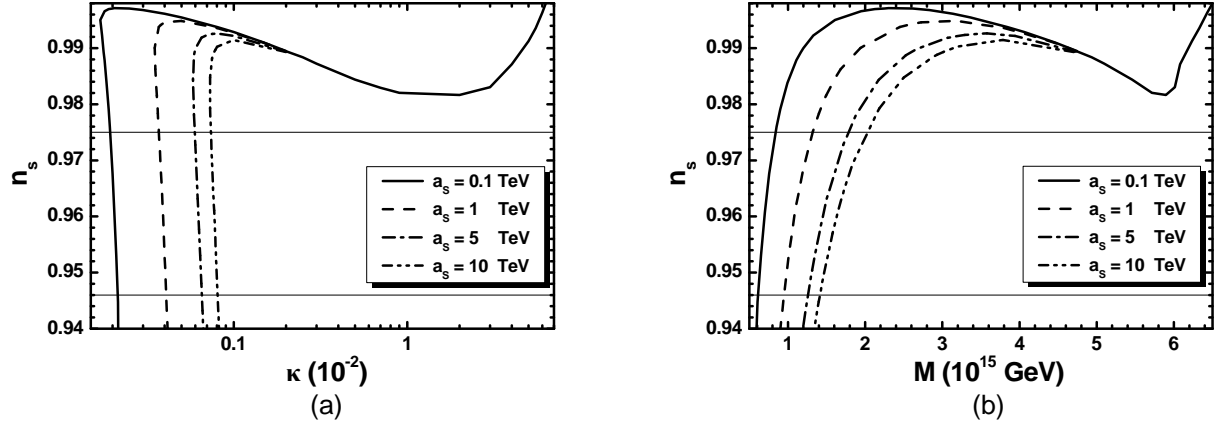


**FIG. 1:**  $n_s$  versus  $\kappa$  (a), and  $n_s$  versus  $M$  (b) for  $a_s = 0.1$  TeV (solid lines),  $a_s = 1$  TeV (dashed lines),  $a_s = 5$  TeV (dot-dashed lines) and  $a_s = 10$  TeV (double dot-dashed lines). The two horizontal lines are based on Eq. (13a)

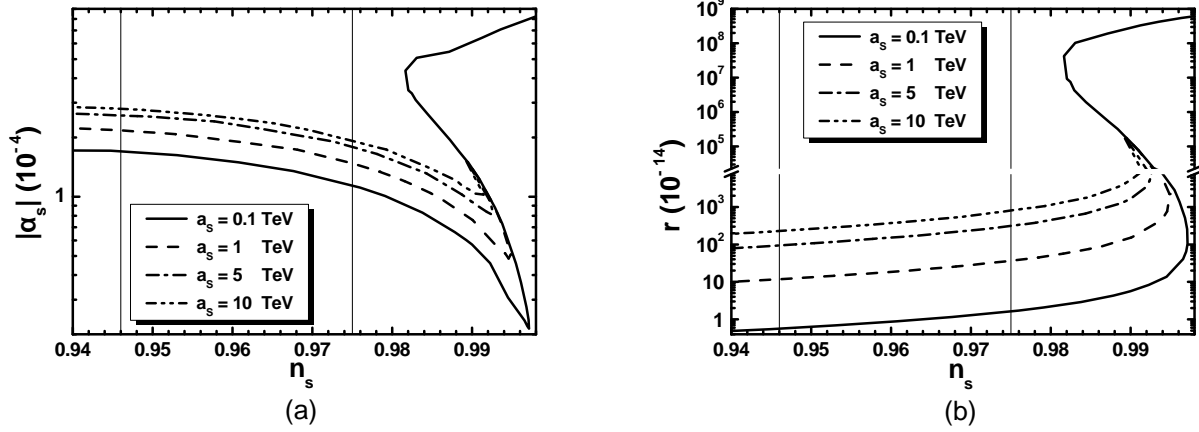


**FIG. 2:**  $|\alpha_s|$  versus  $n_s$  (a), and  $r$  versus  $n_s$  (b) respectively. Vertical lines arise from Eq. (13a).

4. **RESULTS.** The investigation of our model depends on the parameters:

$$\kappa, M, a_s, T_{\text{rh}}, \text{ and } \sigma_*.$$

In our computation, we use as input parameters  $a_s$  and  $\kappa$ , and fix  $T_{\text{rh}} \simeq 5 \cdot 10^8$  GeV, as suggested by our results in Sec. III. Variation of  $T_{\text{rh}}$  over 1–2 orders of magnitude is not expected to significantly alter our findings – see Eq. (9). We then restrict  $M$  and  $\sigma_*$  so that Eqs. (9) and (11) are fulfilled. Using Eqs. (12a) and (12b), we can extract the values for  $n_s$ ,  $\alpha_s$  and  $r$ , thereby testing our model against the observational data of Eqs. (13a) and (13b).

Our results are presented in Figs. 1, 2 and 3 taking  $a_s = 0.1$  TeV (solid lines),  $a_s = 1$  TeV (dashed lines),  $a_s = 5$  TeV (dot-dashed lines), and  $a_s = 10$  TeV (double dot-dashed lines). In Figs. 1 and 2 the observationally compatible region of Eq. (13a) is also indicated by the horizontal (in Fig. 1) or vertical (in Fig. 2) lines. For the sake of clarity, we do not show solutions with  $M > 2 \cdot 10^{16}$  GeV – cf. Ref. [6] – which are totally excluded by Eq. (13a).

From Fig. 1, where we depict  $n_s$  versus  $\kappa$  (a) and  $M$  (b),

we note that, for  $\kappa \gtrsim 0.002$  and  $M \gtrsim 4.7 \cdot 10^{15}$  GeV,  $V_{\text{HIC}}$  and progressively – for  $\kappa \gtrsim 0.04$  and  $M \gtrsim 6.1 \cdot 10^{15}$  GeV, –  $V_{\text{HIS}}$  dominates  $V_{\text{HI}}$  in Eq. (5), and drives  $n_s$  to values close to or larger than 0.98, independently of the selected  $a_s$  values. On the other hand, for  $\kappa \lesssim 0.002$ ,  $V_{\text{HIT}}$  starts becoming comparable to  $V_{\text{HIC}}$  and succeeds in reconciling  $n_s$  with Eq. (13a) for well defined  $\kappa$  (and  $M$ ) values that are related to the chosen  $a_s$ . Actually, for the allowed  $n_s$ , we find that  $V_{\text{HIC}}/V_{\text{HIT}} \simeq 13$ , whereas  $V_{\text{HIS}}$  turns out to be totally negligible. Fixing  $n_s$  to its central value in Eq. (13a), we display in Table I the values for  $(\kappa, M)$  corresponding to the  $a_s$  values employed in Figs. 1-3.

From our numerical computations we observe that, in the regime with acceptable  $n_s$  values, the  $\sigma_*$  required by Eq. (9) becomes comparable to  $\sigma_c$ , and  $f_{\text{rc}}$  in Eq. (6b) can be approximated as [11]

$$f_{\text{rc}}(x) \simeq 3 - \frac{x^{-2}}{6} - \frac{x^{-4}}{30} - \frac{x^{-6}}{84} - \frac{x^{-8}}{180} - \frac{x^{-10}}{330} - \frac{x^{-12}}{546} - \frac{x^{-14}}{840} - \frac{x^{-16}}{1224} - \frac{x^{-18}}{1710} - \frac{x^{-20}}{2310}. \quad (15)$$

**TABLE I:** Model parameters and predictions for  $n_s \simeq 0.96$ .

$a_S$ (TeV)	$\kappa$ ( $10^{-4}$ )	$M$ ( $10^{15}$ GeV)	$\Delta_{c*}$ (%)	$-\alpha_s$ ( $10^{-4}$ )	$r$ ( $10^{-13}$ )
0.1	2.05	0.7	0.6	1.5	0.09
1	3.9	1.2	2	1.9	1.9
5	6.3	1.4	4.3	2.4	15
10	7.7	1.6	6.3	2.5	38

As a consequence,  $V'_{\text{HI}}$ , and therefore  $\epsilon$  in Eq. (10) and  $r$  in Eq. (12b) – see Fig. 2-(b) –, decrease sharply (enhancing  $N_{\text{HI}*}$ ), whereas  $|V''_{\text{HI}}|$  (or  $|\eta|$ ) increases adequately, thereby lowering  $n_s$  within the range of Eq. (13a). In particular, for constant  $\kappa$ , the lower the value for  $n_s$  we wish to attain, the closer we must set  $\sigma_*$  to  $\sigma_c$ . To quantify the amount of this tuning, we define the quantity

$$\Delta_{c*} = (\sigma_* - \sigma_c) / \sigma_c, \quad (16)$$

and list its resulting values in Table I. From there, we conclude that the required tuning is at a few percent level, since  $\Delta_{c*} \leq 10\%$ . Values of  $a_S$  well below 1 TeV are less desirable from this point of view. For comparison, we mention that for  $\kappa \geq 0.002$ , we get  $\Delta_{c*} \geq 30\%$ , i.e.,  $\Delta_{c*}$  increases with  $\kappa$ . From Table I, we note that  $\kappa$  and  $M$  decrease with  $\Delta_{c*}$ , too.

In Fig. 2-(a) and Fig. 2-(b) respectively we display the predictions of our model for  $|\alpha_s| \equiv |dn_s/d \ln k|$  and  $r$ . Corresponding to the  $n_s$  values within Eq. (13a),  $|\alpha_s|$  turns out to be of order  $10^{-4}$ . On the contrast,  $r$  is extremely tiny, of order  $10^{-14} - 10^{-12}$ , and therefore far outside the reach of PLANCK and other contemporary experiments. For the preferred  $n_s$  values, we observe that  $r$  and  $|\alpha_s|$  increase with  $a_S$  whereas for constant  $a_S$ ,  $\alpha_s$ , and  $r$  increase with  $n_s$ . For the  $a_S$  values used in Fig. 2 and with  $n_s = 0.96$ , our predictions are summarized in Table I.

The dependence of  $M$  on  $\kappa$  within our model is shown in Fig. 3. We remark that  $M$  mostly decreases with  $\kappa$ . For low enough  $\kappa$  values, there is region where we get two solutions from Eqs. (9) and (11), for  $M$  and  $\Delta_{c*}$ . Comparing Fig. 3 with Fig. 1-(b), we can easily conclude that the latter solution is consistent with Eq. (13a). The  $M$  values displayed in this figure are fully compatible with the upper bound arising from Eq. (14). Although these  $M$  values lie somewhat below  $M_{\text{GUT}}$ , the unification of gauge coupling constants within MSSM remains intact since the gauge boson associated with the spontaneous  $U(1)_{B-L}$  breaking is neutral under  $G_{\text{MSSM}}$ , and so it does not contribute to the relevant *renormalization group* (RG) running.

As inferred from Fig. 1, for any  $\kappa \lesssim 10^{-4}$  we can conveniently adjust  $a_S$ , so that Eq. (13a) is fulfilled. Working in this direction, we delineate the (lightly gray) region in the  $\kappa - a_S$  [ $M - a_S$ ] plane allowed by all the imposed constraints – see Fig. 4-(a) [Fig. 4-(b)]. We also display by solid lines the allowed contours for  $n_s = 0.96$ . We do not consider  $a_S$  values lower than 0.1 TeV, since they would be less natural from the point of view of both SUSY breaking and the  $\Delta_{c*}$ 's encountered – see Table I. The boundaries of the allowed areas in

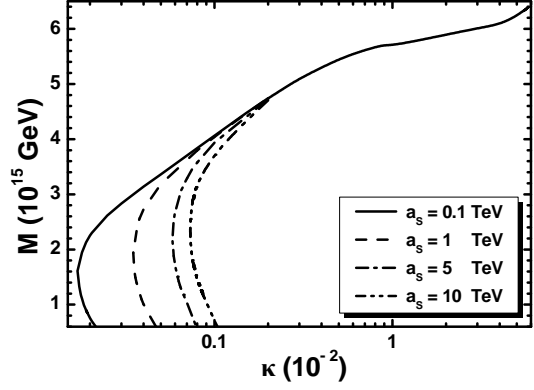
**FIG. 3:**  $M$  versus  $\kappa$  for various  $a_S$  values.

Fig. 4 are determined by the dashed [dot-dashed] lines corresponding to the lower [upper] bound on  $n_s$  in Eq. (13a). In these regions we obtain  $\mu_{\text{cs}} = (0.5 - 6.7) \cdot 10^{-7} m_{\text{P}}^2$  which are compatible with Eq. (14). On the other hand, let us note that these regions are partially compatible with the most stringent (although controversial [28]) constraint  $\mu_{\text{cs}} \lesssim 10^{-7} m_{\text{P}}^2$  [29] imposed by the limit on the stochastic gravitational wave background from the European Pulsar Timing Array. These latter results depend on assumptions regarding string loop formation and the gravitational waves emission. The bounds on  $M$  from  $\mu_{\text{cs}}$ , are totally avoided if we implement FHI within  $G_{\text{LR}}$  [4] or flipped  $SU(5)$  [5], with  $N = 2$  or  $N = 10$  respectively in Eq. (6a), which do not lead to the production of any cosmic defect – for a more complete discussion involving flipped  $SU(5)$  and the corresponding  $M$  values, see second paper in [6].

Summarizing our findings from Fig. 4, for  $n_s$  considered by Eq. (13a) and  $0.1 \lesssim a_S/\text{TeV} \lesssim 10$ , we obtain:

$$1.9 \lesssim \kappa/10^{-4} \lesssim 8.1, \quad 0.85 \lesssim M/10^{15} \text{ GeV} \lesssim 2, \quad (17a)$$

$$1.1 \lesssim |\alpha_s|/10^{-3} \lesssim 2.8, \quad 0.05 \lesssim r/10^{-13} \lesssim 76. \quad (17b)$$

The  $M$  values are consistent with Eq. (14) according to which  $M \lesssim (6.8 - 7.5) \cdot 10^{15} \text{ GeV}$ . The maximal values for  $|\alpha_s|$  and  $r$  are respectively encountered in the upper left and right corners of the allowed region in Fig. 4-(b). In the lower left [right] corner of that area, we obtain the lowest possible  $r$  [ $|\alpha_s|$ ]. Also,  $\Delta_{c*}$  ranges between 0.6% and 7.3%.

### III. NON-THERMAL LEPTOGENESIS

1. **INFLATON DECAY.** As FHI ends,  $\sigma$  crosses  $\sigma_c$ , thereby destabilizing the  $\Phi - \bar{\Phi}$  system which leads to a stage of tachyonic preheating – see Ref. [27]. Soon afterwards, the *inflaton system* (IS) settles into a phase of damped oscillations about the SUSY vacuum, eventually decaying and reheating the universe. Note that the IS consists of the two complex scalar fields  $S$  and  $(\delta\Phi + \delta\bar{\Phi})/\sqrt{2}$ , where  $\delta\Phi = \bar{\Phi} - M$  and  $\delta\bar{\Phi} = \Phi - M$ . To ensure the decay of the IS and implement the see-saw mechanism for the generation of the light neutrino

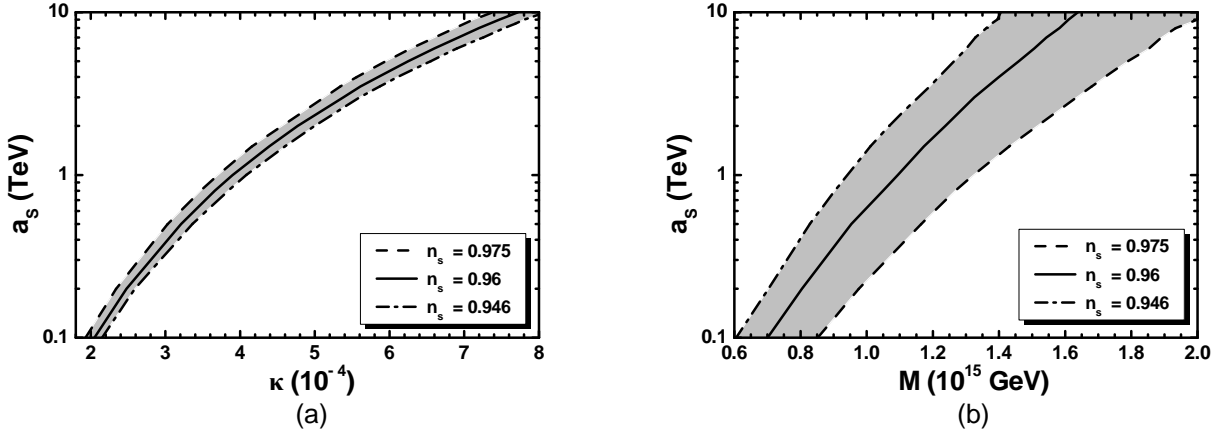


FIG. 4: Allowed (shaded) regions as determined by Eqs. (9), (11), (13a) and (14) in (a)  $\kappa - a_s$  plane and (b)  $M - a_s$  plane. The  $n_s$  values for the various lines are also shown.

masses, we allow for the following superpotential terms:

$$W_{\text{RHN}} = \lambda_i \bar{\Phi} \nu_i^c \nu_i^c + h_{Nij} \nu_i^c L_j H_u, \quad (18)$$

where  $\bar{\Phi} [\nu_i^c]$  have  $B - L$  charge of  $-2[1]$  and  $R$  charge  $0 [\alpha/2]$ .  $L_i$  denotes the  $i$ -th generation  $SU(2)_L$  doublet left-handed lepton superfields, and  $H_u$  is the  $SU(2)_L$  doublet Higgs superfield which couples to the up quark superfields.

At the SUSY vacuum, Eq. (3),  $\Phi$  and  $\bar{\Phi}$  acquire their v.e.v.s, thereby providing masses to the IS and  $\nu_i^c$ 's,

$$(a) \ m_I = \sqrt{2}\kappa M \text{ and } (b) \ M_{i\nu^c} = 2\lambda_i M. \quad (19)$$

The predominant decay channels of  $S$  and  $(\delta\bar{\Phi} + \delta\Phi)/\sqrt{2}$  are to (kinematically allowed) bosonic and fermionic  $\nu_i^c$ 's respectively via tree-level couplings derived from Eqs. (1) and (18) – see e.g. Ref. [23] – with almost the same decay width [26]

$$\Gamma_{I \rightarrow \nu_i^c} = \frac{1}{64\pi} \lambda_i^2 m_I \sqrt{1 - 4M_{i\nu^c}^2/m_I^2}. \quad (20)$$

We assume here that the  $\mu$  problem of MSSM is resolved as suggested in Ref. [5, 31], rather than by invoking the mechanism of Ref. [4] which would open new and efficient decay channels for  $S$ . The SUGRA-induced [32] decay channels are negligible in our set-up, with the  $M$  and  $m_I$  values in Eq. (17a). The resulting reheating temperature is given by [30]

$$T_{\text{rh}} \approx (72/5\pi^2 g_*)^{1/4} \sqrt{\sum_i \Gamma_{I \rightarrow \nu_i^c} m_P}, \quad (21)$$

where  $g_* = 228.75$  counts the MSSM effective number of relativistic degrees of freedom at temperature  $T_{\text{rh}}$ .

For  $T_{\text{rh}} < M_{i\nu^c}$ , the out-of-equilibrium decay of  $\nu_i^c$  generates a lepton-number asymmetry (per  $\nu_i^c$  decay),  $\varepsilon_i$ . The resulting lepton-number asymmetry is partially converted through sphaleron effects into a yield of the observed BAU:

$$Y_B = -0.35 \cdot 2 \cdot \frac{5 T_{\text{rh}}}{4 m_I} \sum_i \text{Br}_i \varepsilon_i, \text{ with } \text{Br}_i = \frac{\Gamma_{I \rightarrow \nu_i^c}}{\sum_i \Gamma_{I \rightarrow \nu_i^c}} \quad (22)$$

being the branching ratio of IS to  $\nu_i^c$ . The quantity  $\varepsilon_i$  can be expressed in terms of the Dirac masses of  $\nu_i$ ,  $m_{iD}$ , arising from the second term of Eq. (18).

The required  $T_{\text{rh}}$  in Eq. (22) must be compatible with constraints on the gravitino ( $\tilde{G}$ ) abundance,  $Y_{3/2}$ , at the onset of nucleosynthesis (BBN), which is estimated to be [18]:

$$Y_{3/2} \simeq 1.9 \cdot 10^{-22} T_{\text{rh}}/\text{GeV}, \quad (23)$$

where we take into account only thermal production of  $\tilde{G}$ , and assume that  $\tilde{G}$  is much heavier than the MSSM gauginos – the case of  $\tilde{G}$  CDM was recently analyzed in Ref. [27].

2. POST-INFLATIONARY REQUIREMENTS. The success of our post-inflationary scenario can be judged, if, in addition to the constraints of Sec. II, it is consistent with the following requirements:

- The bounds on  $M_{i\nu^c}$ :

$$M_{i\nu^c} \lesssim 7.1M, \ M_{1\nu^c} \gtrsim 10T_{\text{rh}} \text{ and } m_I \geq 2M_{i\nu^c}, \quad (24)$$

for some  $\nu_i^c$ 's. The first bound comes from the needed perturbativity of  $\lambda_i$ 's in Eq. (18), i.e.  $\lambda_i \leq \sqrt{4\pi}$ . The second inequality is applied to avoid any erasure of the produced  $Y_L$  due to  $\nu_1^c$  mediated inverse decays and  $\Delta L = 1$  scatterings [36]. Finally, the last bound above ensures a kinematically allowed decay of the IS for some  $\nu_i^c$ 's.

- Constraints from Neutrino Physics. We take as inputs the best-fit values [19] – see also Ref. [20] – on the neutrino mass-squared differences,  $\Delta m_{21}^2 = 7.62 \cdot 10^{-3} \text{ eV}^2$  and  $\Delta m_{31}^2 = (2.55 [-2.43]) \cdot 10^{-3} \text{ eV}^2$ , on the mixing angles,  $\sin^2 \theta_{12} = 0.32$ ,  $\sin^2 \theta_{13} = 0.0246 [0.025]$ , and  $\sin^2 \theta_{23} = 0.613 [0.6]$  and the CP-violating Dirac phase  $\delta = 0.8\pi [-0.03\pi]$  for *normal [inverted] ordered* (NO [IO]) *neutrino masses*,  $m_{i\nu}$ 's. The sum of  $m_{i\nu}$ 's is bounded from above by the data [13, 15],  $\sum_i m_{i\nu} \leq 0.28 \text{ eV}$  at 95% c.l.

- The observational results on  $Y_B$  [13, 15]

$$Y_B \simeq (8.55 \pm 0.217) \cdot 10^{-11} \text{ at 95\% c.l.} \quad (25)$$

**TABLE II:** Parameters yielding the correct BAU for  $\kappa = 0.00039$ ,  $a_S = 1$  TeV and various neutrino mass schemes.

Parameters	Cases						
	A	B	C	D	E	F	G
	Normal Hierarchy		Degenerate Masses			Inverted Hierarchy	
Low Scale Parameters							
$m_{1\nu}/0.1\text{ eV}$	0.01	0.1	0.5	0.7	0.7	0.5	0.49
$m_{2\nu}/0.1\text{ eV}$	0.09	0.13	0.51	1.0	0.705	0.51	0.5
$m_{3\nu}/0.1\text{ eV}$	0.5	0.51	0.71	1.12	0.5	0.1	0.05
$\sum_i m_{i\nu}/0.1\text{ eV}$	0.6	0.74	1.7	2.3	1.9	1.1	1
$\varphi_1$	0	$\pi/3$	0	$\pi/2$	0	$-\pi/6$	0
$\varphi_2$	0	0	$\pi/3$	0	$-\pi/2$	0	$-\pi/3$
Leptogenesis-Scale Parameters							
$m_{1D}/0.1\text{ GeV}$	1.67	4.1	3.7	7	7	5	60
$m_{2D}/\text{GeV}$	4	0.5	1.1	1.55	1.03	0.93	4
$m_{3D}/\text{GeV}$	120	120	5	2	2	4	1.32
$M_{1\nu^c}/10^9\text{ GeV}$	2.5	2.4	3.3	6.5	4.6	1	48
$M_{2\nu^c}/10^{10}\text{ GeV}$	47	1.6	1.7	2.7	1.6	2.8	59
$M_{3\nu^c}/10^{12}\text{ GeV}$	3720	580	0.34	0.035	0.046	0.7	10
Decay channels of the Inflaton System, I							
$I \rightarrow$	$\nu_1^c$	$\nu_{1,2}^c$	$\nu_{1,2}^c$	$\nu_{1,2,3}^c$	$\nu_{1,2,3}^c$	$\nu_{1,2}^c$	$\nu_1^c$
Resulting $B$ -Yield							
$10^{11}Y_B^0$	8.9	8.25	8	6	6.9	8.3	11.1
$10^{11}Y_B$	8.5	8.6	8.6	8.6	8.5	8.5	8.6
Resulting $T_{\text{rh}}$ and $\tilde{G}$ -Yield							
$T_{\text{rh}}/10^8\text{ GeV}$	0.7	2	1.9	4.1	5.5	3	5
$10^{14}Y_{3/2}$	1.3	3.8	3.6	9.5	10	6	10

- The bounds on  $Y_{3/2}$  imposed [18] by successful BBN:

$$Y_{3/2} \lesssim \begin{cases} 10^{-14} \\ 4.3 \cdot 10^{-14} \\ 10^{-13} \end{cases} \text{ for } m_{3/2} \simeq \begin{cases} 0.69 \text{ TeV} \\ 8 \text{ TeV} \\ 10.6 \text{ TeV} \end{cases} \quad (26)$$

Here we consider the conservative case where  $\tilde{G}$  decays with a tiny hadronic branching ratio.

**3. RESULTS.** The inflationary requirements of Sec. II restrict  $\kappa$  and  $M$  in the very narrow range presented in Eq. (17a). As a consequence, the mass  $m_I$  of IS given by Eq. (19), is confined to the range  $(2 - 17.8) \cdot 10^{11}$  GeV, and its variation is not expected to decisively influence our results on  $Y_B$ . For this reason, throughout our analysis here we use the central value  $m_I \simeq 6 \cdot 10^{11}$  GeV, corresponding to the second row of Table I.

On the other hand,  $T_{\text{rh}}$  (and  $Y_B$ ) also depend on the masses  $M_{i\nu^c}$  of  $\nu_i^c$  into which the IS decays. Following the bottom-up approach – see Sec. IVB of Ref. [34] –, we find the  $M_{i\nu^c}$ 's

by using as inputs the  $m_{iD}$ 's, a reference mass of the  $\nu_i$ 's –  $m_{1\nu}$  for NO  $m_{i\nu}$ 's, or  $m_{3\nu}$  for IO  $m_{i\nu}$ 's –, the two Majorana phases  $\varphi_1$  and  $\varphi_2$  of the MNS matrix, and the best-fit values mentioned above for the low energy parameters of neutrino physics. In our numerical code, we also estimate, following Ref. [35], the RG evolved values of the latter parameters at the scale of nTL,  $\Lambda_L = m_I$ , by considering the MSSM with  $\tan \beta \simeq 50$  as an effective theory between  $\Lambda_L$  and the SUSY-breaking scale,  $M_{\text{SUSY}} = 1.5$  TeV. We evaluate the  $M_{i\nu^c}$ 's at  $\Lambda_L$ , and we neglect any possible running of the  $m_{iD}$ 's and  $M_{i\nu^c}$ 's. Therefore, we present their values at  $\Lambda_L$ .

Our results are displayed in Table II taking some representative values of the parameters which yield the correct  $Y_B$ , as dictated by Eq. (25). We consider NO (cases A and B), degenerate (cases C, D and E) and IO (cases F and G)  $m_{i\nu}$ 's. In all cases the current limit (see point 2 above) on the sum of  $m_{i\nu}$ 's is safely met – the case D approaches it. The gauge group adopted here,  $G_{B-L}$ , does not predict any relation between the Yukawa couplings constants  $h_N$  entering the second term of Eq. (18) and the other Yukawa couplings in the MSSM. As a consequence, the  $m_{iD}$ 's are free parameters. However, for the sake of comparison, for case A, we take  $m_{3D} = m_t(\Lambda_L)$ , and in case B, we also set  $m_{2D} = m_c(\Lambda_L)$ , where  $m_t$  and  $m_c$  denote the masses of the top and charm quark respectively. We observe that in all cases  $m_{1D} \gtrsim 0.1$  GeV. This is done, in order to fulfill the second inequality in Eq. (24), given that  $m_{1D}$  heavily influences  $M_{1\nu^c}$ . Note that such an adjustment requires theoretical motivation, if the gauge group is  $G_{LR}$  or flipped  $SU(5)$  – cf. Ref. [36].

From Table II we observe that with NO or IO  $m_{i\nu}$ 's, the resulting  $M_{i\nu^c}$ 's are also hierarchical. With degenerate  $m_{i\nu}$ 's, the resulting  $M_{i\nu^c}$ 's are closer to one another. Therefore, in the latter case more IS-decay channels are available, whereas for cases A and G only a single decay channel is open. In all other cases, the dominant contributions to  $Y_B$  arise from  $\varepsilon_2$ . In Table II we also display, for comparison, the  $B$ -yield with ( $Y_B$ ) or without ( $Y_B^0$ ) taking into account the RG effects. We observe that the two results are mostly close to each other with some discrepancies appearing for degenerate and IO  $m_{i\nu}$ 's. Shown also are values for  $T_{\text{rh}}$ , the majority of which are close to  $5 \cdot 10^8$  GeV, and the corresponding  $Y_{3/2}$ 's, which are consistent with Eq. (26) mostly for  $m_{3/2} \gtrsim 8$  TeV. These large values can be comfortably tolerated with the  $a_S$ 's appearing in Fig. 4 for  $A \sim 1$  – see the definition of  $a_S$  below Eq. (8). From the perspective of  $\tilde{G}$  constraint, case A turns out to be the most promising.

## IV. CONCLUSIONS

Inspired by the recently released WMAP and PLANCK results for the inflationary observables, we have reviewed and updated the predictions arising from a minimal model of SUSY (F-term) hybrid inflation, also referred to as FHI. In this set-up [1], FHI is based on a unique renormalizable superpotential, employs a canonical Kähler potential, and is associated with a superheavy  $B - L$  phase transition. As shown in Ref. [6], and verified by us here, to achieve  $n_s$  values lower

than 0.98, one should include in the inflationary potential the soft SUSY breaking tadpole term, with the SUSY breaking mass parameter values in the range  $(0.1 - 10)$  TeV. Fixing  $n_s$  to its central value, the dimensionless coupling constant, the  $B - L$  symmetry breaking scale, and the inflationary parameters  $\alpha_s$  and  $r$  are respectively given by  $\kappa = (2 - 7.7) \cdot 10^{-4}$ ,  $M = (0.7 - 1.6) \cdot 10^{15}$  GeV,  $|\alpha_s| \simeq (1.5 - 2.5) \cdot 10^{-4}$  and  $r \simeq (0.1 - 37) \cdot 10^{-13}$ . The  $B - L$  cosmic strings, formed at the end of FHI, have tension ranging from 0.7 to  $4.55 \cdot 10^{-7} m_p^2$  and may be accessible to future observations. We have also

briefly discussed the reheating temperature, gravitino constraints and non-thermal leptogenesis taking into account updated values for the neutrino oscillation parameters.

#### ACKNOWLEDGMENTS

Q.S. acknowledges support by the DOE grant No. DE-FG02-12ER41808.

#### REFERENCES

- [1] G.R. Dvali, Q. Shafi and R.K. Schaefer, *Phys. Rev. Lett.* **73**, 1886 (1994) [hep-ph/9406319].
- [2] E.J. Copeland *et al.*, *Phys. Rev. D* **49**, 6410 (1994) [astro-ph/9401011].
- [3] V.N. Şenoğuz and Q. Shafi, hep-ph/0512170.
- [4] G.R. Dvali, G. Lazarides and Q. Shafi, *Phys. Lett. B* **424**, 259 (1998) [hep-ph/9710314].
- [5] B. Kyae and Q. Shafi, *Phys. Lett. B* **635**, 247 (2006) [hep-ph/0510105].
- [6] M.U. Rehman, Q. Shafi and J.R. Wickman, *Phys. Lett. B* **683**, 191 (2010) [arXiv:0908.3896]; M. U. Rehman, Q. Shafi and J. R. Wickman, *Phys. Lett. B* **688**, 75 (2010) [arXiv:0912.4737]; M. Civate, M. U. Rehman, E. Sabo, Q. Shafi and J. Wickman, arXiv:1303.3602.
- [7] A.D. Linde and A. Riotto *Phys. Rev. D* **56**, 1841 (1997) [hep-ph/9703209]; V.N. Şenoğuz and Q. Shafi, *Phys. Lett. B* **567**, 79 (2003) [hep-ph/0305089].
- [8] V.N. Şenoğuz and Q. Shafi, *Phys. Rev. D* **71**, 043514 (2005) [hep-ph/0412102].
- [9] M. Bastero-Gil, S.F. King, and Q. Shafi, *Phys. Lett. B* **651**, 345 (2007) [hep-ph/0604198]; B. Garbrecht *et al.*, *J. High Energy Phys.* **12**, 038 (2006) [hep-ph/0605264]; M.U. Rehman, V.N. Şenoğuz, and Q. Shafi, *Phys. Rev. D* **75**, 043522 (2007) [hep-ph/0612023]; C. Pallis, *J. Cosmol. Astropart. Phys.* **04**, 024 (2009) [arXiv:0902.0334].
- [10] M.U. Rehman, Q. Shafi and J.R. Wickman, *Phys. Rev. D* **83**, 067304 (2011) [arXiv:1012.0309].
- [11] R. Armillis and C. Pallis, “Recent Advances in Cosmology”, edited by A. Travena and B. Soren (Nova Science Publishers Inc., New York, 2013) [arXiv:1211.4011].
- [12] G. Lazarides and C. Pallis, *Phys. Lett. B* **651**, 216 (2007) [hep-ph/0702260].
- [13] G. Hinshaw *et al.* [WMAP Collaboration], arXiv:1212.5226.
- [14] P.A.R. Ade *et al.* [Planck Collaboration], arXiv:1303.5082.
- [15] P.A.R. Ade *et al.* [Planck Collaboration], arXiv:1303.5076.
- [16] G. Lazarides and Q. Shafi, *Phys. Lett. B* **258**, 305 (1991); K. KumeKawa, T. Moroi and T. Yanagida, *Prog. Theor. Phys.* **92**, 437 (1994) [hep-ph/9405337]; G. Lazarides, R.K. Schaefer and Q. Shafi, *Phys. Rev. D* **56**, 1324 (1997) [hep-ph/9608256]; V.N. Şenoğuz and Q. Shafi, *Phys. Rev. D* **71**, 043514 (2005) [hep-ph/0412102].
- [17] M. Yu. Khlopov and A.D. Linde, *Phys. Lett. B* **138**, 265 (1984); J. Ellis, J.E. Kim, and D.V. Nanopoulos, *ibid.* **145**, 181 (1984).
- [18] M.Kawasaki, K.Kohri and T. Moroi, *Phys. Lett. B* **625**, 7 (2005) [astro-ph/0402490]; M. Kawasaki, K. Kohri and T. Moroi, *Phys. Rev. D* **71**, 083502 (2005) [astro-ph/0408426]; R.H. Cyburt *et al.*, *Phys. Rev. D* **67**, 103521 (2003) [astro-ph/0211258]; J.R. Ellis, K.A. Olive and E. Vangioni, *Phys. Lett. B* **619**, 30 (2005) [astro-ph/0503023].
- [19] D.V. Forero, M. Tortola and J.W.F. Valle, *Phys. Rev. D* **86**, 073012 (2012) [arXiv:1205.4018].
- [20] G.L. Fogli *et al.*, *Phys. Rev. D* **86**, 013012 (2012) [arXiv:1205.5254].
- [21] P.A.R. Ade *et al.* [Planck Collaboration], arXiv:1303.5085.
- [22] M. Hindmarsh, *Prog. Theor. Phys. Suppl.* **190**, 197 (2011) [arXiv:1106.0391]; D.M. Regan, arXiv:1112.5899 and references therein.
- [23] G. Lazarides, *Lect. Notes Phys.* **592**, 351 (2002) [hep-ph/0111328]; G. Lazarides, *J. Phys. Conf. Ser.* **53**, 528 (2006) [hep-ph/0607032].
- [24] D.H. Lyth and A. Riotto, *Phys. Rept.* **314**, 1 (1999) [hep-ph/9807278]; A. Mazumdar and J. Rocher, *Phys. Rept.* **497**, 85 (2011) [arXiv:1001.0993].
- [25] J. Rocher and M. Sakellariadou, *J. Cosmol. Astropart. Phys.* **03**, 004 (2005) [hep-ph/0406120]; R. Jeannerot and M. Postma, *J. High Energy Phys.* **05**, 071 (2005) [hep-ph/0503146].
- [26] K. Nakayama *et al.*, *J. Cosmol. Astropart. Phys.* **12**, 010 (2010) [arXiv:1007.5152].
- [27] W. Buchmuller, V. Domcke and K. Schmitz, *Nucl. Phys.* **B862**, 587 (2012) [arXiv:1202.6679].
- [28] S.A. Sanidas, R.A. Battye and B. W. Stappers, *Phys. Rev. D* **85**, 122003 (2012) [arXiv:1201.2419].
- [29] R. van Haasteren *et al.*, arXiv:1103.0576.
- [30] C. Pallis, *Nucl. Phys.* **B751**, 129 (2006) [hep-ph/0510234].
- [31] G. Lazarides and Q. Shafi, *Phys. Rev. D* **58**, 071702 (1998) [hep-ph/9803397].
- [32] M. Endo, F. Takahashi and T.T. Yanagida, *Phys. Rev. D* **76**, 083509 (2007) [arXiv:0706.0986].
- [33] M. Bolz, A. Brandenburg and W. Buchmüller, *Nucl. Phys.* **B606**, 518 (2001); M. Bolz, A. Brandenburg and W. Buchmüller, *Nucl. Phys.* **B790**, 336 (2008) (E) [hep-ph/0012052]; J. Pradler and F.D. Steffen, *Phys. Rev. D* **75**, 023509 (2007) [hep-ph/0608344].
- [34] C. Pallis and Q. Shafi, *Phys. Rev. D* **86**, 023523 (2012) [arXiv:1204.0252].
- [35] S. Antusch, J. Kersten, M. Lindner and M. Ratz, *Nucl. Phys.* **B674**, 401 (2003) [hep-ph/0305273].
- [36] V.N. Şenoğuz, *Phys. Rev. D* **76**, 013005 (2007) [arXiv:0704.3048].